Chinese Journal of Aeronautics, 2013,26(3): 751–765

Chinese Society of Aeronautics and Astronautics
& Beihang University

Chinese Journal of Aeronautics

cja@buaa.edu.cn
www.sciencedirect.com

Codes cross-correlation analysis and data/pilot code pairs optimization for Galileo E1 OS and GPS L1C

Yang Zaixiu, Huang Zhigang *, Geng Shengqun

School of Electronic and Information Engineering, Beihang University, Beijing 100191, China

Received 10 January 2012; revised 6 March 2012; accepted 28 May 2012
Available online 30 April 2013

KEYWORDS

Code cross-correlation;
Code pair optimization;
Galileo;
Global positioning system;
Multiplexed binary offset carrier;
S-curve bias

Abstract The Galileo E1 open service (OS) and the global positioning system (GPS) L1C are intending to use the multiplexed binary offset carrier (MBOC) modulation in E1/L1 band, including both pilot and data components. The impact of data and pilot codes cross-correlation on the distortion of the discriminator function (i.e., the S-curve) is investigated, when only the pilot (or data) components of MBOC signals are tracked. It is shown that the modulation schemes and the receiver configuration (e.g., the correlator spacing) strongly affect the S-curve bias. In this paper, two methods are proposed to optimize the data/pilot code pairs of Galileo E1 OS and GPS L1C. The optimization goal is to obtain the minimum average S-curve bias when tracking only the pilot components a the specific correlator spacing. Figures of merit, such as S-curve bias, correlation loss and code tracking variance have been adopted for analyzing and comparing the un-optimized and optimized code pairs. Simulation results show that the optimized data/pilot code pairs could significantly mitigate the intra-channel codes cross-correlation, and then improve the code tracking performance of MBOC signals.

1. Introduction

Global navigation satellite systems (GNSSs) become increasingly important in a growing number of applications. The new modulations that will be used for the modernized global positioning system (GPS) L1C and Galileo E1 open service (OS) signals have drawn a lot of attention over the past several years. These new signals result from an agreement between the European Commission and the United States of America (USA) in order to use the common multiplexed binary offset carrier (MBOC) signal baseline, with the aim of assuring the compatibility and interoperability between GPS and Galileo systems.[1] MBOC might be thought of as a variant of binary offset carrier (BOC) modulation. For the GPS L1C signal, the USA has chosen the time-multiplexed BOC (TMBOC) solution,[2] while the composite BOC (CBOC) is the implementation selected for the Galileo E1 OS signal.[3]

Pseudo random noise (PRN) codes are a fundamental element in any code division multiple access (CDMA) system such as GPS, Galileo and Compass. In fact, these codes are the tool that enables a GNSSs receiver to distinguish one satellite from another.[4] The Galileo E1 OS will broadcast for the first time so-called random codes, which are codes optimized

* Corresponding author. Tel.: +86 10 82339618.
E-mail addresses: yangzaixiu_cxy@126.com (Z. Yang), baahzg@163.com (Z. Huang), gengshengqun@163.com (S. Geng).

Peer review under responsibility of Editorial Committee of CJA.

Production and hosting by Elsevier

1000-9361 © 2013 Production and hosting by Elsevier Ltd. on behalf of CSAA & BUAA. Open access under CC BY-NC-ND license.
http://dx.doi.org/10.1016/j.cja.2013.04.033

in a highly multidimensional space to make them as random as possible. The idea of the patented random codes is presented in Ref. 5. However Galileo is not alone in bringing new concept into the world of GNSSs. The GPS L1C signal will also make use of the new structure of codes based on the so-called Weil sequences, which will be applied for the very first time in navigation. A complete discussion of the Weil-based codes for GPS L1C can be found in Refs. 6,7.

For the optimization of the Galileo codes, different metrics were employed to account for the different users Galileo would be targeting in the future, as discussed in Ref. 8. Additionally, Ref. 8 analyzed the code performance during the signal acquisition and tracking phases separately. The selected PRN code sets of Galileo E1 OS, as well as the codes of GPS L1C, are presented in detail and their generation mechanisms are analyzed in Ref. 9. The properties of both code families in terms of even and odd auto-correlation and cross-correlation are shown and compared. Moreover, the detailed analysis of inter-system cross-correlation between Galileo E1 OS and GPS L1C has been presented in Ref. 9. The codes cross-correlation impact on the interference vulnerability of MBOC signals is analyzed in Ref. 10, based on a new family of curves, called interference error envelope (IEE).[11]

In previous literature, the code families of each particular band were optimized taking into account only code properties. This means that the real modulation characteristics of the signal, i.e., its particular spreading waveform and multiplex, were not considered in the code design. In fact, the derived codes of MBOC signals would be optimal only in the wide sense if the data and pilot signals were transmitted in quadrature.[12] However, as we know from the GPS and Galileo interface control documents (ICDs),[2,3] the data and pilot components constituting the MBOC signals are transmitted in phase.

In this paper, the impact of data and pilot codes cross-correlation on code tracking performance is measured by the S-curve bias. Two approaches for optimizing the data/pilot code pairs, based on current codes in the GPS and Galileo ICDs, are introduced. Analysis shows that the currently published MBOC codes could still be further optimized to decrease data and pilot codes cross-correlation, and thus a further increase of performance is still achievable in this regard.

2. MBOC signals and cross-correlation functions

The GPS L1C and Galileo E1 OS will transmit a common modulation signal—MBOC(6,1,1/11), where (6,1) refers to the BOC(6,1) part that is added with BOC(1,1) and 1/11 denotes the percentage of power of BOC(6,1) with respect to the total MBOC signal power.[13] For the GPS L1C signal, the USA has chosen the TMBOC solution that multiplexes a BOC(1,1) with a BOC(6,1) in time domain, while the CBOC is the implementation selected for the Galileo E1 OS signal.

The modernized GPS L1C signal will include two channels: the data channel, transmitted using the BOC(1,1) modulation and with 25% of the total power, and the pilot channel, representing 75% of the total power and taking advantage of the TMBOC(6,1,4/33) modulation. The spreading time series of TMBOC(6,1,4/33) comprises 29/33 BOC(1,1) components and 4/33 BOC(6,1) components.[2] On the other hand, the Galileo E1 OS signal will be transmitted by splitting the power equally between data and pilot channels and using the CBOC(6,1,1/11) modulation. It must be remarked that the different sign combination of BOC(1,1) and BOC(6,1) subcarriers for the data channel (denoted as CBOC(+)) and the pilot channel (denoted as CBOC(−)) is foreseen in the Galileo ICD.[3]

Different code families (i.e., the random codes for Galileo E1 OS and the Weil codes for GPS L1C) will be used in tiered code structures featuring different lengths, as summarized in Table 1.

Because the impact of codes cross-correlation is evaluated in the worst case scenario where the signs of the data message and the secondary code are the same, the message and the secondary code may not essentially affect the following analysis results, and are ignored in this paper.

The baseband spread spectrum signal can then be written as[14]

$$c(t) = \sum_{k=-\infty}^{\infty} a[k]p(t - kT_c) \tag{1}$$

where $a[k]$ is the spreading sequence with a period of N, and $p(t)$ is the spreading symbol with a duration time of T_c. Obviously, $c(t)$ is pseudorandom waveform with a period of NT_c. For CBOC(+)/CBOC(−) signals, $p(t)$ is the weighted sum/difference of BOC(1,1) and BOC(6,1) spreading symbols. However, for TMBOC, $p(t)$ is time-multiplexed spreading symbols of BOC(1,1) and BOC(6,1).

Now we focus on the auto-correlation function (ACF) and cross-correlation function (CCF) of MBOC signals. In order to obtain the CCF expression, we introduce

$$\begin{cases} c_1(t) = \sum_{k=-\infty}^{\infty} a_1[k]p_1(t - kT_c) \\ c_2(t) = \sum_{k=-\infty}^{\infty} a_2[k]p_2(t - kT_c) \end{cases} \tag{2}$$

where $a_1[k]$ and $a_2[k]$ are the spreading sequences (i.e., the PRN code sequences) with the same period of N, and $p_1(t)$ and $p_2(t)$ are the spreading symbols with the same duration time of T_c.

The CCF of $c_1(t)$ and $c_2(t)$ is defined as[14]

$$R_{c_1/c_2}(\tau) = \frac{1}{NT_c}\int_0^{NT_c} c_1(t+\tau)c_2(t)\mathrm{d}t \tag{3}$$

Substituting Eq. (2) into Eq. (3) yields

$$R_{c_1/c_2}(\tau) = \frac{1}{NT_c}\sum_{k=-\infty}^{\infty}\sum_{n=-\infty}^{\infty} a_1[k]a_2[n] \times \int_0^{NT_c} p_1(t+\tau - kT_c)p_2(t - nT_c)\mathrm{d}t \tag{4}$$

By letting $k = n + m$, one can obtain

$$R_{c_1/c_2}(\tau) = \frac{1}{NT_c}\sum_{m=-\infty}^{\infty}\sum_{n=-\infty}^{\infty} a_1[n+m]a_2[n] \times \int_0^{NT_c} p_1(t+\tau - (n+m)T_c)p_2(t - nT_c)\mathrm{d}t \tag{5}$$

Table 1 Galileo E1 OS and GPS L1C PRN codes.

Signal	Channel	Code length (chip)		Code type	Tiered code length (ms)
		Primary	Secondary		
E1 OS	B(data)	4092	–	Random	4
	C(pilot)	4092	25		100
L1C	D(data)	10,230	–	Weil	10
	P(pilot)	10,230	1800		18,000

Considering that $p_1(t)$ and $p_2(t)$ are nonzero for $t \in [0, T_c)$, Eq. (5) becomes

$$R_{c_1/c_2}(\tau) = \frac{1}{NT_c}\sum_{m=-\infty}^{\infty}\sum_{n=0}^{N-1} a_1[n+m]a_2[n] \times \int_0^{NT_c} p_1(t+\tau - (n+m)T_c)p_2(t-nT_c)\mathrm{d}t \quad (6)$$

For $0 \leqslant n < N$, the integral of Eq. (6) can then be expressed as

$$\begin{aligned} &1/T_c \times \int_0^{NT_c} p_1(t+\tau-(n+m)T_c)p_2(t-nT_c)\mathrm{d}t \\ &= 1/T_c \times \int_{-\infty}^{\infty} p_1(t+\tau-(n+m)T_c)p_2(t-nT_c)\mathrm{d}t \\ &= R_{p_1/p_2}(\tau - mT_c) \end{aligned} \quad (7)$$

where $R_{p_1/p_2}(\tau)$ is the normalized cross-correlation function of $p_1(t)$ and $p_2(t)$.

Substituting Eq. (7) into Eq. (6) yields

$$\begin{aligned} R_{c_1/c_2}(\tau) &= \frac{1}{N}\sum_{m=-\infty}^{\infty}\sum_{n=0}^{N-1} a_1[n+m]a_2[n]R_{p_1/p_2}(\tau - mT_c) \\ &= \sum_{m=-\infty}^{\infty} R_{a_1/a_2}[m]R_{p_1/p_2}(\tau - mT_c) \end{aligned} \quad (8)$$

where $R_{a_1/a_2}[m]$ is the discrete cross-correlation function of $a_1[k]$ and $a_2[k]$,

$$R_{a_1/a_2}[m] = \frac{1}{N}\sum_{n=0}^{N-1} a_1[n+m]a_2[n] \quad (9)$$

Eq. (8) shows that the CCF of $c_1(t)$ and $c_2(t)$ is determined by the CCFs of the spreading sequences ($a_1[k]$ and $a_2[k]$) and the spreading symbols ($p_1(t)$ and $p_2(t)$). Obviously, $R_{c_1/c_2}(\tau)$ is periodic within the period of NT_c. In fact, that is why GNSSs code correlation properties are analyzed by circular correlation rather than linear correlation.[9]

From Eq. (8), the ACF of $c(t)$ can be written as

$$R_c(\tau) = \sum_{m=-\infty}^{\infty} R_a[m]R_p(\tau - mT_c) \quad (10)$$

In fact, of particular concern in the paper is the main lobe of the CCF (i.e., $R_{c_1/c_2}(\tau)$ for $\tau \in [-T_c, T_c]$), which will affect the discriminator functions of GNSSs signals. Eq. (8) indicates that the main lobe is determined by $R_{a_1/a_2}[-1]R_{p_1/p_2}(\tau + T_c)$, $R_{a_1/a_2}[0]R_{p_1/p_2}(\tau)$ and $R_{a_1/a_2}[1]R_{p_1/p_2}(\tau - T_c)$. For example, if $R_{p_1/p_2}(\tau)$ is even symmetric and $R_{a_1/a_2}[-1] = R_{a_1/a_2}[1]$, the main lobe of $R_{c_1/c_2}(\tau)$ would be even symmetric.

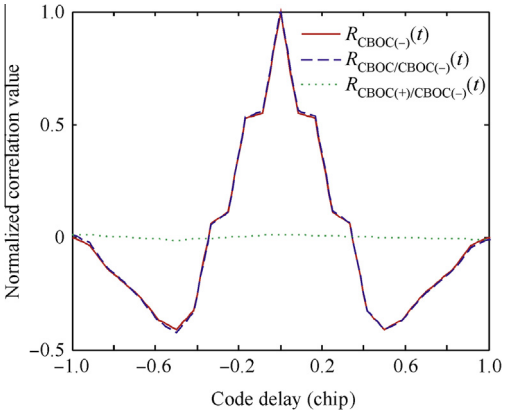

Fig. 1 Cross-correlation functions of CBOC signals.

From the above description, we can obtain the CCFs of CBOC signals for Galileo E1 OS PRN1 shown in Fig. 1. 2 As already seen, the ACF of CBOC(−) (RCBOC(−)(τ)) is symmetric. It can be noted that the CCF of the CBOC (data and pilot together) signal and the pilot signal ($R_{CBOC/CBOC(-)}(\tau)$) is not symmetric, due to the asymmetry of the data and pilot CCF ($R_{CBOC(+)/CBOC(-)}(\tau)$). In the following section, the impact of the asymmetric CCF on the S-curve bias is discussed in detail.

3. Codes cross-correlation impact on S-curve bias

In this section the impact of codes cross-correlation on the S-curves of MBOC signals is discussed. Both Galileo E1 OS and GPS L1C signals are taken into account, with the specific analysis on how different code families can affect the S-curve bias. Moreover, the architectural choice and several parameters, including the tracking algorithm, the correlator spacing and the discriminator type, are also considered.

3.1. S-curve bias

The navigation receiver obtains the (noise-less) code delay by the zero-crossing of the code discriminator function (i.e., the S-curve). Considering coherent early-late processing (CELP), the S-curve, based on the CCF $R_{c_1/c_2}(\tau)$, can be defined as[15]

$$S_C(\varepsilon, \Delta) = R_{c_1/c_2}(\varepsilon + \Delta/2) - R_{c_1/c_2}(\varepsilon - \Delta/2) \quad (11)$$

with its lock-point $\varepsilon_{bias}(\Delta)$ defined by

$$S_C(\varepsilon_{bias}(\Delta), \Delta) = 0 \quad (12)$$

where Δ is the early-late spacing (i.e., the correlator spacing), ε is the code delay, and $\varepsilon_{bias}(\Delta)$ represents the S-curve bias.

Considering that Δ is within the interval of $(0, T_c]$, $\varepsilon_{bias}(\Delta)$ is determined by the main lobe of $R_{c_1/c_2}(\tau)$. If the main lobe of $R_{c_1/c_2}(\tau)$ is even symmetric (e.g., $R_c(\tau)$), we have the relationship

$$\begin{aligned} S_C(-\varepsilon, \Delta) &= R_{c_1/c_2}(\varepsilon - \Delta/2) - R_{c_1/c_2}(\varepsilon + \Delta/2) \\ &= -S_C(\varepsilon, \Delta) \end{aligned} \quad (13)$$

In other words, the S-curve is an odd function, which guarantees that $\varepsilon_{bias}(\Delta)$ is zero for $0 < \Delta \leqslant T_c$.

However, as mentioned above, the main lobe of $R_{c_1/c_2}(\tau)$ is even symmetric only when special requirements are satisfied. In practice, when only the pilot (or data) components of Galileo E1 OS and GPS L1C signals are tracked, it is very difficult to exactly satisfy these requirements. The S-curve bias caused by the codes cross-correlation for Galileo E1 OS and GPS L1C signals is considered and analyzed in Sections 3.2 and 3.3.

3.2. Galileo E1 OS

For the matched processing of the CBOC (data and pilot channels together) signal, the S-curve bias is zero. This is due fact that the ACF is even symmetric. In order to evaluate the impact of the codes cross-correlation on the S-curve, let us consider tracking Galileo E1 OS signals by using only the pilot components (denoted as CBOC/CBOC(−)) or only the data components (denoted as CBOC/CBOC(+)).

The corresponding S-curves for Galileo E1 OS PRN1 codes are depicted in Fig. 2, with the CELP discriminator, an early-late spacing of 1 chip and infinite bandwidth. It is clear that the CBOC/CBOC(−) and CBOC/CBOC(+) methods would result in S-curve biases of 0.0225 chip and −0.0045 chip, respectively. The biases are due to the codes cross-correlation of data and pilot channels and the fact that data and pilot components are transmitted in phase. It is possible to notice that the codes cross-correlation properties could lead to an asymmetric S-curve in case of receiving a single channel (e.g., the pilot channel).

It is well known that the S-curve bias result in the pseudorange error. However, according to the basic principle of GNSSs positioning, the positioning accuracy would not degrade if the S-curve biases of visible satellites visible are the same. The S-curve biases caused by codes cross-correlation for all Galileo E1 OS signals are shown in Fig. 3 under the same conditions as in Fig. 2. It can be clearly seen that the S-curve biases are not the same for different satellites. Thus, the codes cross-correlation effect cannot be neglected in positioning solution. The maximum bias is about 12.8 m for CBOC/CBOC(−), but 2.7 m for CBOC/CBOC(+). In this case, the CBOC/CBOC(+) method outperform the CBOC/CBOC(−) method.

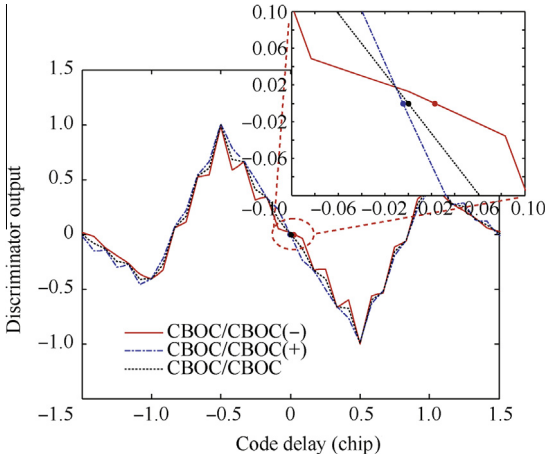

Fig. 2 S-curves and its zoom of the CBOC signal.

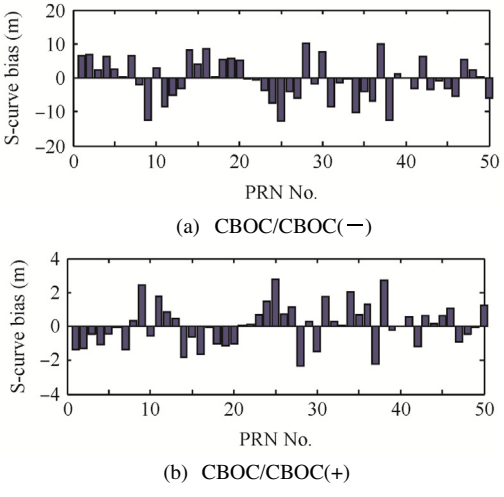

Fig. 3 S-curve biases of Galileo E1 OS PRN1∼50.

To further investigate the impact of the codes cross-correlation, Fig. 4 shows the average S-curve biases of CBOC signals using the arbitrary spacing, with CELP and non-coherent early-late processing (NELP)[16] discriminators. The average S-curve bias is obtained from the absolute S-curve biases of all CBOC signals for the specific early-late spacing. It can be observed that the CBOC/CBOC(+) is potentially less sensitive to the early-late spacing than the CBOC/CBOC(−). In other words, the CBOC(+) provides improvement of the resistance to codes cross-correlation, as compared to the CBOC(−). Moreover, it is noted that the S-curve biases of CELP are remarkably similar to NELP except for the CBOC/CBOC(+) at the spacing of near 0.7 chip.

In addition to the tracking methods mentioned above, MBOC signals can also be tracked with the BOC(1,1) receiver[17] and the TM61 receiver.[18] In Fig. 5, the impact of the codes cross-correlation on the average S-curve biases for CBOC signals with the BOC(1,1) receiver (denoted as CBOC/BOC(1,1)) is reported. In this case, the CBOC(−)/BOC(1,1) provides similar performance to the CBOC(+)/BOC(1,1) for the early-late spacing of less than 0.9 chip. Compared to the CBOC/CBOC(−), the CBOC(−)/BOC(1,1) method significantly reduces the S-curve biases.

Fig. 6 shows the impact of codes cross-correlation on the average S-curve biases for the CBOC/TM61 with the dot product (DP) discriminator.[16] It can be seen that the TM61 method

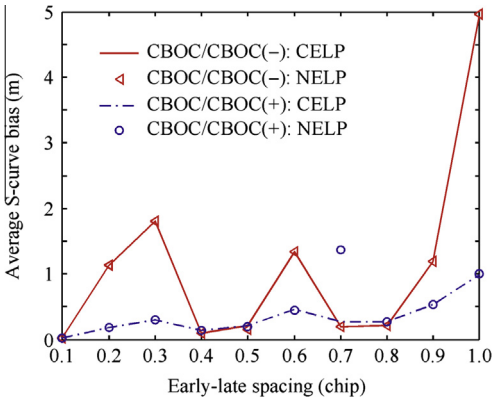

Fig. 4 Average S-curve biases of CBOC signals.

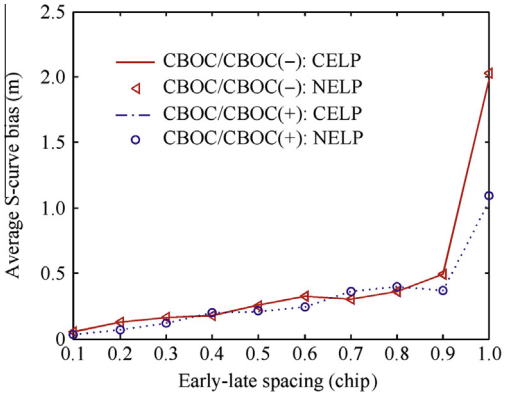

Fig. 5 Average S-curve biases of CBOC/BOC(1,1).

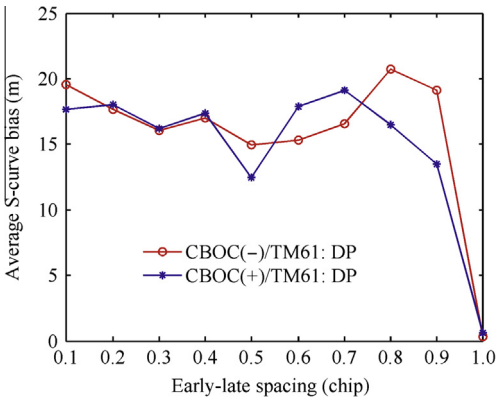

Fig. 6 Average S-curve biases of CBOC/TM61.

introduce serious biases for the early-late spacing of less than 0.9 chip. This is due to the fact that the power of the BOC(6,1) component is very low with respect to the total signal power. Thus, the codes cross-correlation seriously affect the ACF of BOC(6,1). At this point, the TM61 receiver may be not suitable for CBOC signals.

3.3. GPS L1C

In the following, the impact of the codes cross-correlation on the S-curve bias for GPS L1C signals is evaluated. Similar to Galileo E1 OS, the receiver would track only the pilot components (i.e., TMBOC) or the data components (i.e., BOC(1,1)). When tracking only the pilot components, the BOC(1,1) and TM61 receivers are also considered.

When tracking only the pilot component (denoted as GPS-L1C/TMBOC) or the data component (denoted as GPS-L1C/BOC(1,1)), the S-curve biases caused by codes cross-correlation for all GPS L1C signals are shown in Fig. 7, with the CELP discriminator, an early-late spacing of 1 chip and infinite front-end bandwidth. Similar to Galileo E1 OS, the S-curve biases are not the same for different GPS L1C signals and tracking methods.

Fig. 8 shows the impact of codes cross-correlation on the average S-curve biases of GPS L1C signals for different tracking methods, under the same conditions as in Fig. 7. Because the GPS L1C data components are BOC(1,1) signals, only the pilot components can be tracked by the TM61 receiver. Average S-curve biases of GPS L1C for different tracking methods are reported in Fig. 8(a). It should be noted that the GPS L1C pilot signals provide smaller S-curve biases, as compared to the Galileo E1 OS signals (shown in Fig. 4). This is mainly due to the code length of 10,230 chip, which provides better correlation properties than Galileo E1 OS, as well as the power ratio of pilot and data components. Another remark is that the maximum S-curve bias occurs at the early-late spacing of 0.3 chip for GPS-L1C/TMBOC, but 1 chip for CBOC/CBOC(−). It is interesting to note that the relation of the S-curve bias and the early-late spacing for GPS-L1C/BOC(1,1) is approximately linear when the spacing is less than 0.9 chip.

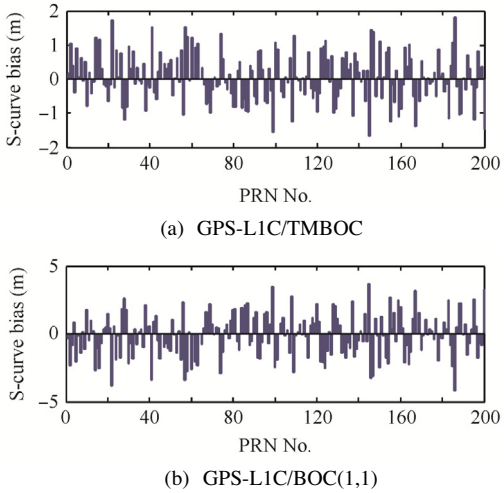

Fig. 7 S-curve biases of GPS L1C signals.

In Fig. 8(b), the impact of codes cross-correlation on the average S-curve biases for TMBOC signals with the BOC(1,1) receiver is shown. In this case, the local reference signal is the enhanced BOC(1,1) signal, which blanks the part of the TMBOC signal modulated by BOC(6,1)[18] in order to reduce the codes cross-correlation. That is why the trend of TMBOC/BOC(1,1) S-curve biases varying with early-late spacings is very similar to GPS-L1C/BOC(1,1). However, the TMBOC/BOC(1,1) method provides smaller S-curve biases than GPS-L1C/BOC(1,1). As regards to the power ratio of GPS L1C pilot and data components, this result is expected.

The average S-curve biases for TMBOC/TM61 with different early-late spacings are reported in Fig. 8(c). Besides the enhanced BOC(1,1) signal, the TMBOC/TM61 method also uses the enhanced BOC(6,1) signal, which blanks the part of the TMBOC signal modulated by BOC(1,1) in order to reduce the codes cross-correlation.[18] As shown in Figs. 6 and 8(c),

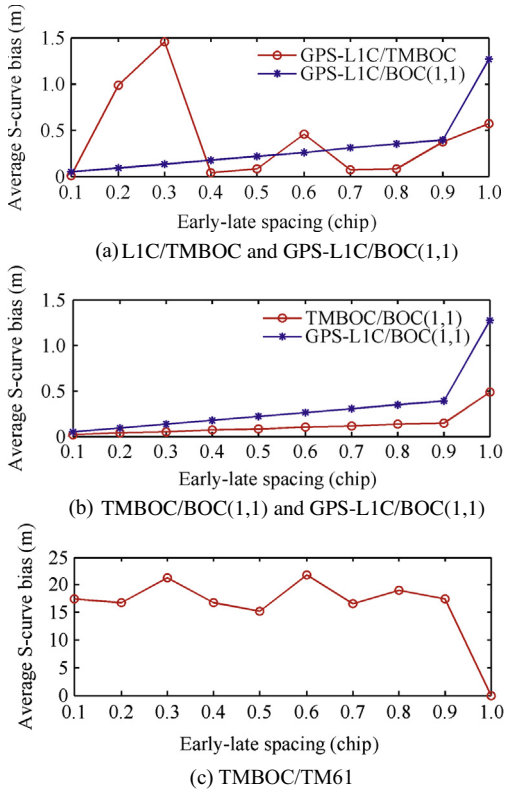

Fig. 8 Average S-curve biases of GPS L1C for different tracking methods.

the TMBOC/TM61 introduces similar S-curve biases to the CBOC/TM61.

From the above discussion, it is evident that the impact of codes cross-correlation on the S-curve bias can be magnified by an inappropriate choice of the early-late spacing, leading to noticeable worsening in receiver performance. When only the pilot components are tracked, GPS L1C provides smaller average S-curve biases, as compared to Galileo E1 OS, due to the differences the code length and the power proportion between data and pilot components.

4. Data/pilot code pairs optimization

As mentioned above, the data and pilot codes cross-correlation results in the S-curve bias for Galileo E1 OS and GPS L1C, which directly degrades the code tracking performance. Based on the PRN code sets given by Refs. 2,3, two methods are proposed to optimize the data/pilot code pairs of Galileo E1 OS and GPS L1C and then mitigate codes cross-correlation.

Method I: This method reassigns the pilot PRN code number, generating new data/pilot PRN code pairs, but maintains the data and pilot PRN code groups given by the GPS and Galileo ICDs.[2,3]

Method II: This method regroups the PRN codes given by the GPS and Galileo ICDs,[2,3]generating new data/pilot PRN code pairs.

In some studies, it has been shown that the modernized pilot channel would significantly improve the resistance of the code tracking loop to thermal noise,[18] and improve the inherent multipath rejection capability of MBOC signals.[19] Thus, the optimization goal of the proposed methods is to obtain the minimum average S-curve bias when tracking only the pilot components of Galileo E1 OS (i.e., CBOC/CBOC(−)) and GPS L1C (i.e., GPS-L1C/TMBOC) for a specific early-late spacing. We choose the early-late spacing of 1 chip as the optimization reference for Galileo E1 OS, but 0.3 chip for GPS L1C. As shown in Figs. 4 and 8(a), the maximum average S-curve biases would occur with these spacings. To demonstrate the performance of optimized data/pilot code pairs, several simulation results in terms of S-curve bias, correlation loss and code tracking variance are presented.

4.1. Method I

In this method, the data and pilot PRN code groups given by the GPS and Galileo ICDs[2,3] are not changed, but the pilot PRN code number is reassigned. Then, the new data/pilot PRN code pairs are generated to obtain the minimum average S-curve bias with the specific early-late spacing when only the pilot components are tracked. That is to say, the data and pilot PRN code sequences are consistent with Refs. 2,3, but the pair relationship is changed.

4.1.1. Galileo E1 OS

For Galileo E1 OS, there are 50 data PRN code sequences and 50 pilot PRN code sequences, which are given, respectively, by

$$\boldsymbol{a}^{\mathrm{d}} = \begin{bmatrix} a_1^{\mathrm{d}} & a_2^{d} & \cdots & a_{50}^{\mathrm{d}} \end{bmatrix}, \quad \boldsymbol{a}^{\mathrm{p}} = \begin{bmatrix} a_1^{\mathrm{p}} & a_2^{\mathrm{p}} & \cdots & a_{50}^{\mathrm{p}} \end{bmatrix}^{\mathrm{T}} \tag{14}$$

where a_k^{d} and a_k^{p}, $k = 1, 2, \ldots, 50$ represent the data and pilot No.k PRN code sequences defined in the Galileo ICD, respectively.

In order to generate the optimized data/pilot PRN code pairs, the S-curve biases of possible data/pilot code pairs should be computed for tracking only the pilot components (i.e., CBOC/CBOC(−)). It is convenient to introduce the bias matrix

$$\boldsymbol{B}_{N\times N} = \mathrm{bias}(\boldsymbol{a}^{\mathrm{d}}, \boldsymbol{a}^{\mathrm{p}}) = \begin{bmatrix} \mathrm{bias}\left(a_1^{\mathrm{d}}, a_1^{\mathrm{p}}\right) & \mathrm{bias}\left(a_1^{\mathrm{d}}, a_2^{\mathrm{p}}\right) & \cdots & \mathrm{bias}\left(a_1^{\mathrm{d}}, a_N^{\mathrm{p}}\right) \\ \mathrm{bias}\left(a_2^{\mathrm{d}}, a_1^{\mathrm{p}}\right) & \mathrm{bias}\left(a_2^{\mathrm{d}}, a_2^{\mathrm{p}}\right) & \cdots & \mathrm{bias}\left(a_2^{\mathrm{d}}, a_N^{\mathrm{p}}\right) \\ \vdots & \vdots & \ddots & \vdots \\ \mathrm{bias}\left(a_N^{\mathrm{d}}, a_1^{\mathrm{p}}\right) & \mathrm{bias}\left(a_N^{\mathrm{d}}, a_2^{\mathrm{p}}\right) & \cdots & \mathrm{bias}\left(a_N^{\mathrm{d}}, a_N^{\mathrm{p}}\right) \end{bmatrix} \tag{15}$$

where $N = 50$, $\left(a_i^{\mathrm{d}}, a_j^{\mathrm{p}}\right)$, $i,j = 1, 2, \ldots, N$ represents the new data/pilot PRN code pair (i.e., a_i^{d} as the data PRN code and a_j^{p} as the pilot PRN code), and $\mathrm{bias}\left(a_i^{\mathrm{d}}, a_j^{\mathrm{p}}\right)$ is the S-curve bias for the code pair $\left(a_i^{\mathrm{d}}, a_j^{\mathrm{p}}\right)$ when only the pilot component is tracked. For Galileo E1 OS, we choose the early-late spacing of 1 chip as the optimization reference. As shown in Fig. 4, the maximum S-curve bias for CBOC/CBOC(−) occurs with the early-late spacing of 1 chip.

Mathematically, the optimization problem is to minimize the cost function[20]

$$z = \sum_{i=1}^{N}\sum_{j=1}^{N} v_{ij}\left|\mathrm{bias}\left(a_i^{\mathrm{d}}, a_j^{\mathrm{p}}\right)\right| \tag{16}$$

where $v_{ij} = \begin{cases} 1, & \left(a_i^{\mathrm{d}}, a_j^{\mathrm{p}}\right)\text{is chosen} \\ 0, & \left(a_i^{\mathrm{d}}, a_j^{\mathrm{p}}\right)\text{is not chosen} \end{cases}$, with the restrictions

(a) $\sum_{i=1}^{N} v_{ij} = 1$, $j = 1, 2, \ldots, N$, i.e., only one element can be chosen in each column of $\boldsymbol{B}$.

(b) $\sum_{j=1}^{N} v_{ij} = 1$, $i = 1, 2, \ldots, N$, i.e., only one element can be chosen in each row of $\boldsymbol{B}$.

Table 2 Galileo E1 OS optimized data/pilot PRN code pairs: Method I.

Type	Data and pilot PRN Codes No.									
Pair/Data	1	2	3	4	5	6	7	8	9	10
Pilot	47	10	32	48	7	6	50	5	22	27
Pair/Data	11	12	13	14	15	16	17	18	19	20
Pilot	15	1	37	8	18	26	44	46	11	4
Pair/Data	21	22	23	24	25	26	27	28	29	30
Pilot	23	34	43	12	39	3	29	38	16	49
Pair/Data	31	32	33	34	35	36	37	38	39	40
Pilot	13	2	33	9	31	20	30	19	36	40
Pair/Data	41	42	43	44	45	46	47	48	49	50
Pilot	42	25	45	41	21	35	24	28	17	14

From the above description, the optimization problem can be modeled as the classic assignment problem in operations research, which can be solved using the Hungarian method.[21]

The optimized data/pilot PRN code pairs are specified in Table 2. The "Pair/Data" rows in Table 2 show the new data/pilot code pair number and the data PRN code number, which are the same as the original data PRN code number given by Ref.3. The "Pilot" rows show the pilot PRN code number given by Ref. 3, which are paired with the data PRN code number of the row above in the same column to generate the new data/pilot code pair. For example, the new pair No.1 is (1,47), where 1 represents the data code number and 47 represents the pilot code number given by Ref. 3. It can be seen that the new pair No.6, 33 and 40 are the same as the original pairs defined in Ref. 3

Comparison of original and optimized data/pilot PRN code pairs is reported in Fig. 9, where the "squares" represent the original code pair relationship defined in the Galileo ICD, and the "circles" represent the optimized code pair relationship. It is clear that the optimized pair relationship seems to be irregular, whereas the original pairs show a linear relationship.

The S-curve biases after the optimization using Method I for all Galileo E1 OS signals are shown in Fig. 10 under the same conditions as in Fig. 3. For both CBOC/CBOC(−) and CBOC/CBOC(+), the S-curve biases decrease significantly, as compared to the un-optimized results (see Fig. 3).

To comprehensively evaluate the performance of method I, the average S-curve biases after optimization for different tracking methods are shown in Fig. 11. For CBOC/CBOC(−), CBOC/CBOC(+), CBOC(−)/ BOC(1,1) and CBOC(+)/ BOC(1,1), Method I provides about 25 dB decrease in the average S-curve biases in comparison to Figs. 4 and 5. It should be noted that, although the optimization criterion of Method I is directly related to the CBOC/CBOC(−) method with the early-late spacing of 1 chip, a significant bias reduction can also be observed for CBOC/CBOC(+), CBOC/BOC(1,1) with different early-late spacings. However, the improvement is not so significant for the TM61 method, and the average biases are still too large for practical applications. Nevertheless, it is concluded that, for Galileo E1 OS, Method I is very effective to mitigate the data and pilot codes cross-correlation.

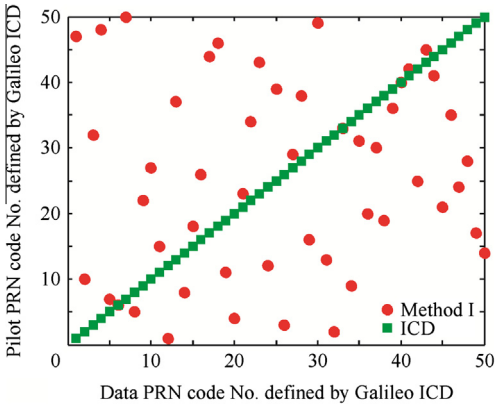

Fig. 9 Comparison of original and optimized data/pilot PRN code pairs of Galileo E1 OS.

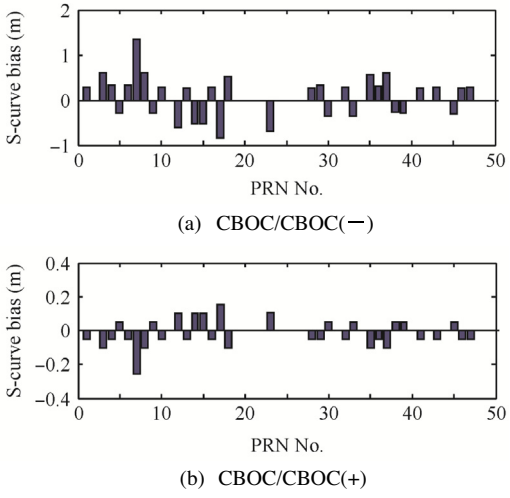

Fig. 10 S-curve biases after optimization for Galileo E1 OS PRN1–50: Method I.

4.1.2. GPS L1C

Similar to Galileo E1 OS, the data and pilot PRN code sequences of GPS L1C are given, respectively, by

$$\boldsymbol{a}^{\mathrm{d}} = \left[a_1^{\mathrm{d}} \quad a_2^{\mathrm{d}} \quad \cdots \quad a_{210}^{\mathrm{d}}\right], \quad \boldsymbol{a}^{\mathrm{p}} = \left[a_1^{\mathrm{p}} \quad a_2^{\mathrm{p}} \quad \cdots \quad a_{210}^{\mathrm{p}}\right]^{\mathrm{T}} \tag{17}$$

Using Eq. (17), we can also obtain the bias matrix of GPS L1C.

For GPS L1C, we choose the early-late spacing of 0.3 chip as the optimization reference, with which the maximum S-curve bias of GPS-L1C/TMBOC occurs (see Fig. 8(a)). The optimization problem is also solved by the Hungarian

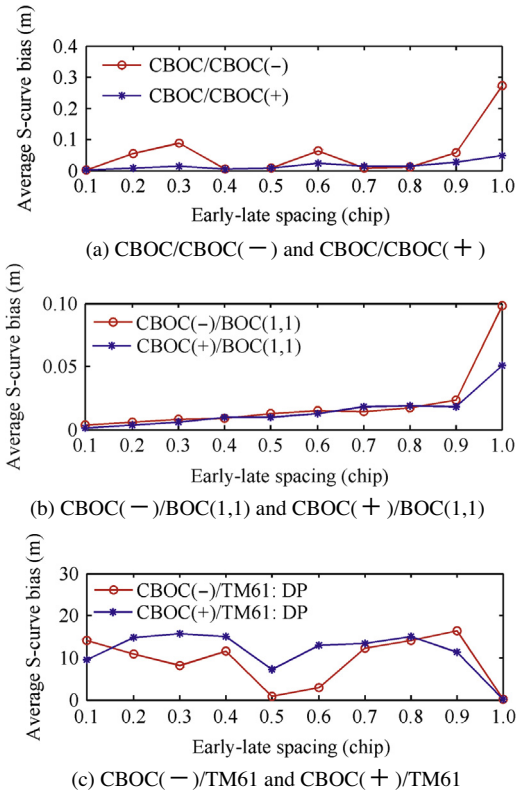

Fig. 11 Average S-curve biases after optimization for Galileo E1 OS: Method I.

Table 3 GPS L1C optimized data/pilot PRN code pairs: Method I.

Type	Data and pilot PRN Codes No.									
Pair/Data	1	2	3	4	5	6	7	8	9	10
Pilot	63	119	127	173	92	198	169	50	32	102
Pair/Data	11	12	13	14	15	16	17	18	19	20
Pilot	81	133	147	79	53	180	171	72	25	123
Pair/Data	21	22	23	24	25	26	27	28	29	30
Pilot	8	125	163	5	34	14	170	18	58	186
Pair/Data	31	32	33	34	35	36	37	38	39	40
Pilot	151	140	139	77	195	56	113	200	189	84
Pair/Data	41	42	43	44	45	46	47	48	49	50
Pilot	104	54	154	187	31	141	136	11	107	115
Pair/Data	51	52	53	54	55	56	57	58	59	60
Pilot	24	9	210	13	30	194	99	130	177	97
Pair/Data	61	62	63	64	65	66	67	68	69	70
Pilot	202	100	4	64	57	109	118	29	86	68
Pair/Data	71	72	73	74	75	76	77	78	79	80
Pilot	17	41	209	124	138	94	46	33	70	44
Pair/Data	81	82	83	84	85	86	87	88	89	90
Pilot	206	120	35	69	1	105	93	114	87	12
Pair/Data	91	92	93	94	95	96	97	98	99	100
Pilot	167	178	176	42	52	60	203	80	75	88
Pair/Data	101	102	103	104	105	106	107	108	109	110
Pilot	48	61	148	128	78	201	51	47	83	66
Pair/Data	111	112	113	114	115	116	117	118	119	120
Pilot	89	156	19	101	106	96	146	132	166	196
Pair/Data	121	122	123	124	125	126	127	128	129	130
Pilot	129	49	117	82	192	193	85	43	73	38
Pair/Data	131	132	133	134	135	136	137	138	139	140
Pilot	179	150	36	98	15	37	184	103	137	116
Pair/Data	141	142	143	144	145	146	147	148	149	150
Pilot	181	62	122	21	207	27	55	160	3	155
Pair/Data	151	152	153	154	155	156	157	158	159	160
Pilot	22	76	134	174	39	153	26	164	162	168
Pair/Data	161	162	163	164	165	166	167	168	169	170
Pilot	28	16	135	126	10	159	144	142	143	165
Pair/Data	171	172	173	174	175	176	177	178	179	180
Pilot	91	90	183	199	185	152	59	131	6	204
Pair/Data	181	182	183	184	185	186	187	188	189	190
Pilot	112	158	2	67	95	172	149	182	108	65
Pair/Data	191	192	193	194	195	196	197	198	199	200
Pilot	74	175	71	23	111	20	191	45	208	190
Pair/Data	201	202	203	204	205	206	207	208	209	210
Pilot	161	110	157	121	205	188	145	7	197	40

method, and the optimized data/pilot PRN code pairs are reported in Table 3. The ''Pair/Data'' rows show the new data/pilot pair number and the data PRN code number, which are the same as the original data PRN code number in Ref. 2. The ''Pilot'' rows show the pilot PRN code number given by Ref. 2, which are paired with the data PRN code number of the row above in the same column to generate the new data/pilot code pair. For example, the new pair No.1 is (1,63), where 1 represents the data PRN code number and 63 represents the pilot code number given by Ref. 2.

The average S-curve biases after the optimization for different tracking methods are shown in Fig. 12. Compared to Fig. 8(a) and (b), Method I effectively mitigates the codes cross-correlation. However, unlike Galileo E1 OS, the early-late spacing strongly impacts the optimization gain for GPS-L1C/TMBOC, GPS-L1C/BOC(1,1) and TMBOC/BOC(1,1).

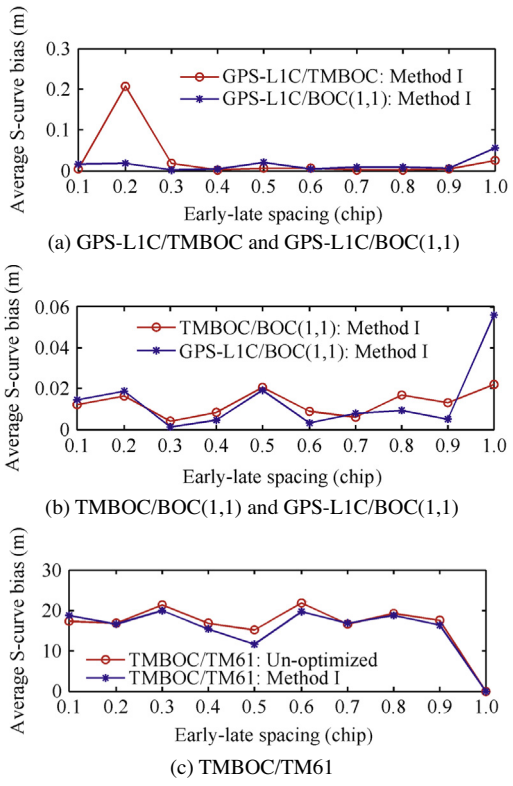

Fig. 12 Average S-curve biases after optimization for GPS L1C: Method I.

For example, the optimization gain for GPS-L1C/TMBOC is approximately 38 dB for $\Delta = 0.3$ chip (the optimization reference spacing), but around 13.5 dB for $\Delta = 0.2$ chip. Thus, the reference early-late spacing is a critical parameter for optimizing the GPS L1C code pairs, and should be selected carefully. It is noted that, after optimization, the relation between the S-curve bias and the early-late spacing for GPS-L1C/BOC(1,1) and TMBOC/BOC(1,1) is non-linear, as compared to Fig. 8(b). Similar to CBOC/TM61, Method I may have very limited effect on TMBOC/TM61.

4.2. Method II

In this method, the data and pilot PRN code groups given by Refs. 2,3 are changed, and the PRN code number is reassigned. That is to say, the total PRN code sequences are consistent with Refs. 2,3, but the PRN code groups (i.e., data or pilot) and the pair relationship may be changed. Then, the new data/pilot PRN code pairs are generated, to obtain the minimum average S-curve bias with a specific early-late spacing when only the pilot components are tracked.

4.2.1. Galileo E1 OS

For Galileo E1 OS, there are 100 PRN code sequences, which are regrouped and renumbered. New data and pilot PRN code vectors are, respectively, defined as

$$\boldsymbol{a}^{\mathrm{d}} = \left[a_1^{\mathrm{d}} \quad a_2^{\mathrm{d}} \quad \cdots \quad a_N^{\mathrm{d}} \quad a_1^{\mathrm{p}} \quad a_2^{\mathrm{p}} \quad \cdots \quad a_N^{\mathrm{p}}\right], \quad \boldsymbol{a}^{\mathrm{p}} = (\boldsymbol{a}^{\mathrm{d}})^{\mathrm{T}} \tag{18}$$

where $N = 50$, and a_k^{d} and a_k^{p}, $k = 1, 2, \ldots, N$ represent the data and pilot No.k PRN code sequences defined in the Galileo ICD,[3] respectively.

In order to generate the optimized data/pilot PRN code pairs, the S-curve biases of possible data/pilot code pairs should be computed for tracking only the pilot components (i.e., CBOC/CBOC(−)). Similar to method I, the bias matrix is given by

$$\begin{aligned}\boldsymbol{B}_{2N\times 2N} &= [b_{ij}]_{2N\times 2N} = \mathrm{bias}(\boldsymbol{a}^{\mathrm{d}}, \boldsymbol{a}^{\mathrm{p}}) \\ &= \begin{bmatrix} \mathrm{bias}(a_1^{\mathrm{d}}, a_1^{\mathrm{d}}) & \mathrm{bias}(a_1^{\mathrm{d}}, a_2^{\mathrm{d}}) & \cdots & \mathrm{bias}(a_1^{\mathrm{d}}, a_N^{\mathrm{p}}) \\ \mathrm{bias}(a_2^{\mathrm{d}}, a_1^{\mathrm{d}}) & \mathrm{bias}(a_2^{\mathrm{d}}, a_2^{\mathrm{d}}) & \cdots & \mathrm{bias}(a_2^{\mathrm{d}}, a_N^{\mathrm{p}}) \\ \vdots & \vdots & \ddots & \vdots \\ \mathrm{bias}(a_N^{\mathrm{p}}, a_1^{\mathrm{d}}) & \mathrm{bias}(a_N^{\mathrm{p}}, a_2^{\mathrm{d}}) & \cdots & \mathrm{bias}(a_N^{\mathrm{p}}, a_N^{\mathrm{p}}) \end{bmatrix}\end{aligned} \tag{19}$$

In fact, the main diagonal elements of $\boldsymbol{B}$ are impossible to occur, because one code sequence cannot simultaneously belong to the data and pilot channels. Moreover, $\boldsymbol{B}$ is antisymmetric (i.e.,$\boldsymbol{B} = -\boldsymbol{B}^{\mathrm{T}}$), which is proved in the following.

Let a_1 and a_2 represent a_k^{d} or a_k^{p}, $k = 1, 2, \ldots, N$, and $a_1 \neq a_2$. For the data/pilot code pair (a_1,a_2), by considering Eq. (1), the CBOC(−) and CBOC(+) can be written, respectively, as

$$\begin{cases} c_{\mathrm{CBOC}(+),1}(t) = \alpha c_{\mathrm{BOC}(1,1),1}(t) + \beta c_{\mathrm{BOC}(6,1),1}(t) \\ c_{\mathrm{CBOC}(-),2}(t) = \alpha c_{\mathrm{BOC}(1,1),2}(t) - \beta c_{\mathrm{BOC}(6,1),2}(t) \end{cases} \tag{20}$$

with $\alpha = \sqrt{10/11}$, $\beta = \sqrt{1/11}$, and

$$\begin{cases} c_{\mathrm{BOC}(1,1),i}(t) = \sum\limits_{k=-\infty}^{\infty} a_i[k] p_{\mathrm{BOC}(1,1)}(t - kT_{\mathrm{c}}), \quad i = 1, 2 \\ c_{\mathrm{BOC}(6,1),i}(t) = \sum\limits_{k=-\infty}^{\infty} a_i[k] p_{\mathrm{BOC}(6,1)}(t - kT_{\mathrm{c}}), \quad i = 1, 2 \end{cases} \tag{21}$$

where $p_{\mathrm{BOC}(1,1)}(t)$ and $p_{\mathrm{BOC}(6,1)}(t)$ represent the spreading symbols of BOC(1,1) and BOC(6,1), respectively.

From Eq. (3), the CCF of CBOC and CBOC(−) can be written as

$$R_{\mathrm{CBOC/CBOC}(-),2}(\tau) = R_{c_{\mathrm{CBOC}(+),1}/c_{\mathrm{CBOC}(-),2}}(\tau) + R_{c_{\mathrm{CBOC}(-),2}}(\tau) \tag{22}$$

where $R_{c_{\mathrm{CBOC}(+),1}/c_{\mathrm{CBOC}(-),2}}(\tau)$ is the CCF of $c_{\mathrm{CBOC}(+),1}(t)$ and $c_{\mathrm{CBOC}(-),2}(t)$. Using Eq. (8), $R_{c_{\mathrm{CBOC}(+),1}/c_{\mathrm{CBOC}(-),2}}(\tau)$ can be expressed as

$$\begin{aligned} R_{c_{\mathrm{CBOC}(+),1}/c_{CBOC(-),2}}(\tau) = \sum_{m=-\infty}^{\infty} R_{a_1/a_2}[m] \times \Big(&\alpha^2 R_{p_{\mathrm{BOC}(1,1)}}(\tau - mT_{\mathrm{c}}) \\ &- \alpha\beta R_{p_{\mathrm{BOC}(1,1)}/p_{\mathrm{BOC}(6,1)}}(\tau - mT_{\mathrm{c}}) \\ &+ \alpha\beta R_{p_{\mathrm{BOC}(6,1)}/p_{\mathrm{BOC}(1,1)}}(\tau - mT_{\mathrm{c}}) \\ &+ \beta^2 R_{p_{\mathrm{BOC}(6,1)}}(\tau - mT_{\mathrm{c}})\Big) \end{aligned} \tag{23}$$

Similarly, for the data/pilot code pair (a_2,a_1), the CCF of CBOC and CBOC(−) can be expressed as

$$R_{\mathrm{CBOC/CBOC}(-),1}(\tau) = R_{c_{\mathrm{CBOC}(+),2}/c_{\mathrm{CBOC}(-),1}}(\tau) + R_{c_{\mathrm{CBOC}(-),1}}(\tau) \tag{24}$$

with

$$\begin{aligned} R_{c_{\mathrm{CBOC}(+),2}/c_{\mathrm{CBOC}(-),1}}(\tau) = \sum_{m=-\infty}^{\infty} R_{a_2/a_1}[m] \times \Big(&\alpha^2 R_{p_{\mathrm{BOC}(1,1)}}(\tau - mT_{\mathrm{c}}) \\ &- \alpha\beta R_{p_{\mathrm{BOC}(1,1)}/p_{\mathrm{BOC}(6,1)}}(\tau - mT_{\mathrm{c}}) \\ &+ \alpha\beta R_{p_{\mathrm{BOC}(6,1)}/p_{\mathrm{BOC}(1,1)}}(\tau - mT_{\mathrm{c}}) \\ &+ \beta^2 R_{p_{\mathrm{BOC}(6,1)}}(\tau - mT_{\mathrm{c}})\Big) \end{aligned} \tag{25}$$

As shown in Ref. 9, the random codes of Galileo E1 OS fulfill the autocorrelation sidelobe zero (ASZ) property (i.e.,

$R_{a_1}[-1] = R_{a_1}[1] = R_{a_2}[-1] = R_{a_2}[1] = 0$). From Eq. (10), the following relationship can be derived

$$R_{c_{\mathrm{CBOC}(-),1}}(\tau) = R_{c_{\mathrm{CBOC}(-),2}}(\tau), \quad -T_c \leqslant \tau \leqslant T_c \tag{26}$$

Moreover, it can be easily proved that $R_{p_{\mathrm{BOC}(1,1)}/p_{\mathrm{BOC}(6,1)}}(\tau)$ is an even function.

Let ε_1 and ε_2 denote bias(a_1,a_2) and bias (a_2,a_1), respectively. As mentioned above, ε_1 and ε_2 are determined by the main lobes of $R_{\mathrm{CBOC/CBOC}(-),2}(\tau)$ and $R_{\mathrm{CBOC/CBOC}(-),1}$ (τ), respectively. Using Eqs. (11) and (12), we can obtain

$$R_{\mathrm{CBOC/CBOC}(-),2}\left(\varepsilon_1 + \frac{\Delta}{2}\right) - R_{\mathrm{CBOC/CBOC}(-),2}\left(\varepsilon_1 - \frac{\Delta}{2}\right) = 0 \tag{27}$$

Using Eqs. (26) and (27), the following relationship can be derived

$$R_{\mathrm{CBOC/CBOC}(-),1}\left(-\varepsilon_1 - \frac{\Delta}{2}\right) - R_{\mathrm{CBOC/CBOC}(-),1}\left(-\varepsilon_1 + \frac{\Delta}{2}\right) = 0 \tag{28}$$

Due to ε_2 = bias(a_2,a_1), we can obtain

$$R_{\mathrm{CBOC/CBOC}(-),1}\left(\varepsilon_2 + \frac{\Delta}{2}\right) - R_{\mathrm{CBOC/CBOC}(-),1}\left(\varepsilon_2 - \frac{\Delta}{2}\right) = 0 \tag{29}$$

Combining Eqs. (28) and (29) gives

$$\varepsilon_2 = -\varepsilon_1 \tag{30}$$

That is bias (a_1,a_2) = −bias(a_2,a_1). Therefore, $\boldsymbol{B}$ is antisymmetric (i.e.,$\boldsymbol{B} = -\boldsymbol{B}^{\mathrm{T}}$). In other words, for two PRN code sequences, the absolute S-curve biases of CBOC signals are the same, no matter which one is defined as the data PRN code.

Obviously, the Hungarian method cannot be directly applied to $|\boldsymbol{B}|$ to generate the optimized data/pilot PRN code pairs. In order to ensure that the diagonal elements of $\boldsymbol{B}$ are not chosen, we introduce a modified bias matrix

$$\boldsymbol{B}' = |\boldsymbol{B}| + \lambda \boldsymbol{I} \tag{31}$$

where $\boldsymbol{I}$ is the identity matrix, and λ is a positive big enough (e.g., $\lambda > \sum_{i=1}^{2N}\sum_{j=1}^{2N}|b_{ij}|$).

Then, using the Hungarian method, we can obtain 100 elements which are symmetric to the main diagonal of $\boldsymbol{B}'$, due to the fact that $\boldsymbol{B}'$ is a symmetric matrix. By arbitrarily choosing one from the two elements symmetric with respect to the main diagonal, we can obtain 50 elements, which correspond to the new data/pilot PRN code pairs. Clearly, the optimized data/pilot PRN code pairs would not be unique.

For simplicity, we choose the 50 elements from the upper triangular part of $\boldsymbol{B}'$. The results are reported in Table 4. The "Pair" rows show the number of new data/pilot pairs. The "Data" rows show the PRN code number in Ref. 3, and the corresponding PRN code belongs to the data channel after optimization. The "Pilot" rows show the PRN code number in Ref. 3, which is paired with the data PRN code number of the row above in the same column, to generate the new data/pilot code pair. And the corresponding PRN code belongs to the pilot channel after optimization. The postfix "d" the data channel, and "p" indicates that the PRN code originally belongs to the pilot channel in Ref. 3. For example, the new pair No.3 is (3d,8p), where "3d" indicates the data PRN code number and "8p" indicates the pilot code number in Ref. 3. Similar to Table 2, the new pair No.6, 33 and 40 are the same as the original pairs defined in Ref. 3.

Comparison of the average S-curve biases obtained by using different optimization methods and tracking algorithms is shown in Fig. 13. For CBOC/CBOC(−) and CBOC/CBOC(+), the improvement of Method II has been shown to be around 8 dB (see Fig. 13(a)), as compared to Method I. The similar performance improvement can also be observed for CBOC/BOC(1,1) (see Fig. 13(b)). Compared to the results of method I, the average S-curve biases of Method II for CBOC/TM61 further decrease, but they are still too large in contrast with other tracking algorithms. As regards to the principles of the proposed methods, these results are expected.

4.2.2. GPS L1C

For GPS L1C, there are 420 PRN code sequences, which are regrouped and renumbered. New data and pilot code vectors are defined, respectively, as

Table 4 Galileo E1 OS optimized data/pilot PRN code pairs: Method II.

Type	Data and pilot PRN Codes No.									
Pair	1	2	3	4	5	6	7	8	9	10
Data	1d	3p	3d	4d	5d	6d	7d	8d	9d	10d
Pilot	2d	5p	8p	41d	29d	6p	15d	16d	13p	50d
Pair	11	12	13	14	15	16	17	18	19	20
Data	11d	12d	13d	14d	4p	7p	17d	18d	19d	20d
Pilot	15p	11p	39d	22d	26p	44p	32d	30d	46p	49p
Pair	21	22	23	24	25	26	27	28	29	30
Data	21d	16p	23d	24d	25d	26d	27d	28d	17p	20p
Pilot	23p	50p	14p	12p	39p	1p	29p	38p	30p	31p
Pair	31	32	33	34	35	36	37	38	39	40
Data	31d	22p	33d	34d	24p	36d	37d	38d	32p	40d
Pilot	19p	47p	33p	35d	27p	49d	2p	10p	42p	40p
Pair	41	42	43	44	45	46	47	48	49	50
Data	34p	42d	43d	44d	45d	46d	47d	48d	36p	37p
Pilot	48p	25p	9p	41p	21p	35p	18p	28p	43p	45p

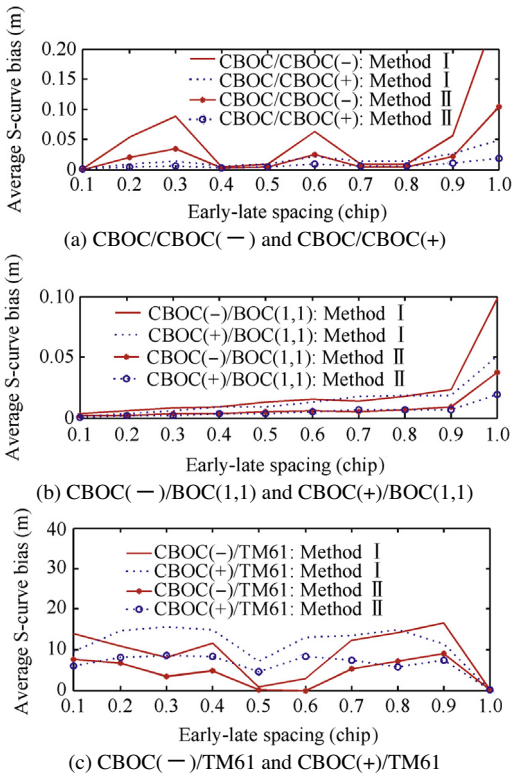

Fig. 13 Comparison of average S-curve biases obtained by using different optimization methods for E1 OS.

$$\boldsymbol{a}^{\mathrm{d}} = \begin{bmatrix} a_1^{\mathrm{d}} & a_2^{\mathrm{d}} & \cdots & a_N^{\mathrm{d}} & a_1^{\mathrm{p}} & a_2^{\mathrm{p}} & \cdots & a_N^{\mathrm{p}} \end{bmatrix}, \quad \boldsymbol{a}^{\mathrm{p}} = (\boldsymbol{a}^{\mathrm{d}})^{\mathrm{T}} \tag{32}$$

where $N = 210$, and a_k^{d} and a_k^{p}, $k = 1, 2, \ldots, N$ represent the data and pilot No.k PRN code sequences defined in the GPS ICD,[2] respectively.

Similar to Galileo E1 OS, the bias matrix is given by

$$\boldsymbol{B}_{2N\times 2N} = [b_{ij}]_{2N\times 2N} = \mathrm{bias}(\boldsymbol{a}^{\mathrm{d}}, \boldsymbol{a}^{\mathrm{p}}) = \begin{bmatrix} \mathrm{bias}(a_1^{\mathrm{d}}, a_1^{\mathrm{d}}) & \mathrm{bias}(a_1^{\mathrm{d}}, a_2^{\mathrm{d}}) & \cdots & \mathrm{bias}(a_1^{\mathrm{d}}, a_N^{\mathrm{p}}) \\ \mathrm{bias}(a_2^{\mathrm{d}}, a_1^{\mathrm{d}}) & \mathrm{bias}(a_2^{\mathrm{d}}, a_2^{\mathrm{d}}) & \cdots & \mathrm{bias}(a_2^{\mathrm{d}}, a_N^{\mathrm{p}}) \\ \vdots & \vdots & \ddots & \vdots \\ \mathrm{bias}(a_N^{\mathrm{p}}, a_1^{\mathrm{d}}) & \mathrm{bias}(a_N^{\mathrm{p}}, a_2^{\mathrm{d}}) & \cdots & \mathrm{bias}(a_N^{\mathrm{p}}, a_N^{\mathrm{p}}) \end{bmatrix} \tag{33}$$

The main diagonal elements of $\boldsymbol{B}$ are impossible to occur, because one code sequence cannot simultaneously belong to the data and pilot channels. However, $\boldsymbol{B}$ is not antisymmetric (or symmetric) for GPS L1C.

In order to generate the optimized data/pilot PRN code pairs, we need to create a new bias matrix $\boldsymbol{B}''$ form $\boldsymbol{B}$. In light of the case of Galileo E1 OS, the matrix $\boldsymbol{B}'' = \left(b_{ij}''\right)_{2N}$ is defined as

$$b_{ij}'' = \begin{cases} \lambda, & i,j = 1,2,\ldots,2N, \quad i = j \\ \min(|b_{ij}|, |b_{ji}|), & i,j = 1,2,\ldots,2N, \quad i \neq j \end{cases} \tag{34}$$

where λ is a positive big enough (e.g., $\lambda > \sum_{i=1}^{2N}\sum_{j=1}^{2N}|b_{ij}|$). Obviously, $\boldsymbol{B}''$ is a symmetric matrix. It is noted that $\boldsymbol{B}''$ is very similar to $\boldsymbol{B}'$ in the case of Galileo E1 OS.

Then, applying the Hungarian method to $\boldsymbol{B}''$, we can obtain 420 elements, which are symmetric to the main diagonal of $\boldsymbol{B}''$. By applying Eq. (34), the expected 210 elements, which correspond to the new data/pilot PRN code pairs, can be easily found. Unlike Galileo E1 OS, the code pairs of GPS L1C optimized by using Method II, are unique.

The data/pilot PRN code pairs optimized by using Method II are given in Table 5. Similar to Table 4, the "Pair" rows show the new data/pilot pair number, and the "Data" and "Pilot" rows show the PRN code number given by GPS ICD.[2] The postfix "d" that the PRN code originally belongs to the data channel, and "p" the pilot channel in the GPS ICD.[2]

Comparison of the average S-curve biases obtained by using different optimization methods and tracking algorithms for GPS L1C is shown in Fig. 14. It is clear that after the optimization Method II the average bias with the early-late spacing of 0.3 chip decreases by 15 dB for GPS-L1C/TMBOC, as compared to Method I. For other early-late spacings, method II outperforms method I slightly. This is mainly due to the fact that the reference early-late spacing for GPS L1C is 0.3 chips. For TMBOC/BOC(1,1) and TMBOC/TM61, Method II provides no significant improvement.

Clearly, Method I and II can significantly mitigate data and pilot (i.e., intra-channel) codes cross-correlation by optimizing the data/pilot code pairs. However, the optimization strategies do not change the inter-channel and inter-system codes cross-correlation properties of Galileo E1 OS and GPS L1C,[9] because the complete PRN code sets of each system are invariant.

4.3. Correlation loss and noise performance of optimized data/pilot code pairs

In the following, the optimized data/pilot code pairs presented above are analyzed in terms of correlation loss and code tracking variance in the presence of thermal noise. The correlation loss can be effectively used to predict the acquisition performance degradation and useful signal power loss (i.e., signal-to-noise ratio (SNR) loss) due to the impact of data and pilot codes cross-correlation. The noise performance of the proposed data/pilot code pairs is evaluated by code tracking variance.

4.3.1. Correlation loss

The correlation loss (due to data and pilot codes cross-correlation) quantifies the real signal power reduction within the correlation process relative to the ideal signal power, which is defined here by[15]

$$C_{\mathrm{L}} = 20\lg\left(\frac{\max\limits_{\tau\in(-T_c,T_c)}(|R_x(\tau)|)}{\max\limits_{\tau\in(-T_c,T_c)}(|R_{y/x}(\tau)|)}\right)\mathrm{dB} \tag{35}$$

where y represents the Galileo E1 OS or GPS L1C signal, and x represents the data or pilot component of y. $R_x(\tau)$ is the ACF of x, and $R_{y/x}(\tau)$ is the CCF of y and x. Due to the relative sign of the data and pilot signals, C_{L} can be positive or negative for each MBOC signal. However, we just consider the positive case which means the CCF has a loss relative to the ACF.

The correlation losses of un-optimized and optimized data/pilot code pairs are compared in Fig. 15 for CBOC/CBOC(−). As expected, the optimization strategies have a significant influence on the correlation loss, except for some specific signals (i.e., PRN6, 33 and 40). The change seems irregular, but

Table 5 GPS L1C optimized data/pilot PRN code pairs: Method II.

Type	Data and pilot PRN Codes No.																			
Pair	1	2	3	4	5	6	7	8	9	10	11	12	13	14	15	16	17	18	19	20
Data	3p	5p	6p	4d	7p	6d	7d	8d	9d	18p	11d	12d	19p	14d	15d	20p	21p	22p	19d	23p
Pilot	16d	125p	157p	153d	82d	2d	178p	114d	143d	3d	81p	86d	210d	134p	53p	22d	160d	202d	74p	142p
Pair	21	22	23	24	25	26	27	28	29	30	31	32	33	34	35	36	37	38	39	40
Data	25p	26p	23d	29p	30p	26d	32p	28d	33p	30d	38p	41p	33d	42p	45p	36d	49p	38d	39d	50p
Pilot	87p	35p	90d	59d	163d	14p	101p	98d	187p	186p	100p	67d	78p	5d	69p	62p	132d	200p	110d	98p
Pair	41	42	43	44	45	46	47	48	49	50	51	52	53	54	55	56	57	58	59	60
Data	41d	51p	55p	56p	57p	46d	58p	48d	59p	50d	63p	52d	65p	66p	55d	67p	57d	58d	68p	70p
Pilot	205d	210p	145p	89p	47p	70d	24p	11p	13p	31d	48p	104d	34p	183p	175d	171p	145	12p	149d	24d
Pair	61	62	63	64	65	66	67	68	69	70	71	72	73	74	75	76	77	78	79	80
Data	61d	62d	71p	64d	65d	66d	72p	68d	69d	77p	71d	80p	82p	74d	75d	76d	77d	78d	79d	80d
Pilot	165d	8p	138d	121d	176d	109p	34d	21d	86p	43d	18d	171d	193d	124p	32d	144d	46p	54d	99d	44p
Pair	81	82	83	84	85	86	87	88	89	90	91	92	93	94	95	96	97	98	99	100
Data	81d	83p	84p	84d	85d	85p	87d	88d	88p	90p	91d	92d	93d	94d	92p	96d	97d	95p	96p	97p
Pilot	15p	52p	4p	44d	1p	63d	95d	114p	132p	91p	37d	25d	118d	169d	20d	60p	27p	40d	179p	154d
Pair	101	102	103	104	105	106	107	108	109	110	111	112	113	114	115	116	117	118	119	120
Data	101d	102d	99p	102p	103p	106d	107d	105p	106p	107p	108p	112d	113d	110p	111p	116d	117d	112p	119d	113p
Pilot	209p	61p	158d	73d	51d	108d	154p	73p	27d	35d	43p	156p	128p	208d	198d	53d	146p	189p	166p	129p
Pair	121	122	123	124	125	126	127	128	129	130	131	132	133	134	135	136	137	138	139	140
Data	115p	122d	123d	124d	117p	126d	118p	120p	129d	121p	131d	122p	133d	134d	135d	136d	137d	130p	139d	140d
Pilot	188p	45d	150d	42d	176p	72d	17p	140p	105d	76p	60d	109d	36p	207d	126p	146d	184p	162d	137p	116p
Pair	141	142	143	144	145	146	147	148	149	150	151	152	153	154	155	156	157	158	159	160
Data	141d	142d	131p	135p	136p	138p	139p	141p	143p	144p	147p	152d	148p	149p	150p	156d	152p	153p	159d	155p
Pilot	181p	155d	147d	103d	120d	123p	197d	100d	56d	184d	49d	128d	16p	196d	54p	127d	183d	167p	13d	111d
Pair	161	162	163	164	165	166	167	168	169	170	171	172	173	174	175	176	177	178	179	180
Data	161d	158p	161p	162p	163p	166d	167d	168d	165p	170d	168p	172d	169p	174d	173p	174p	175p	177p	179d	180d
Pilot	28p	104p	206d	178d	170p	159p	164d	190d	148d	188d	94p	151p	75p	199p	79p	2p	157d	130d	89d	127p
Pair	181	182	183	184	185	186	187	188	189	190	191	192	193	194	195	196	197	198	199	200
Data	181d	182d	180p	182p	185p	190p	187d	191p	192p	193p	191d	192d	194p	194d	195d	195p	196p	198p	199d	200d
Pilot	173d	160p	31p	172p	9p	133p	29d	125d	203p	93p	164p	83d	10d	177d	151d	47d	64p	119p	208p	17d
Pair	201	202	203	204	205	206	207	208	209	210										
Data	201d	201p	203d	204d	202p	204p	205p	206p	209d	207p										
Pilot	115d	10p	185d	1d	40p	39p	189d	197p	186d	37p										

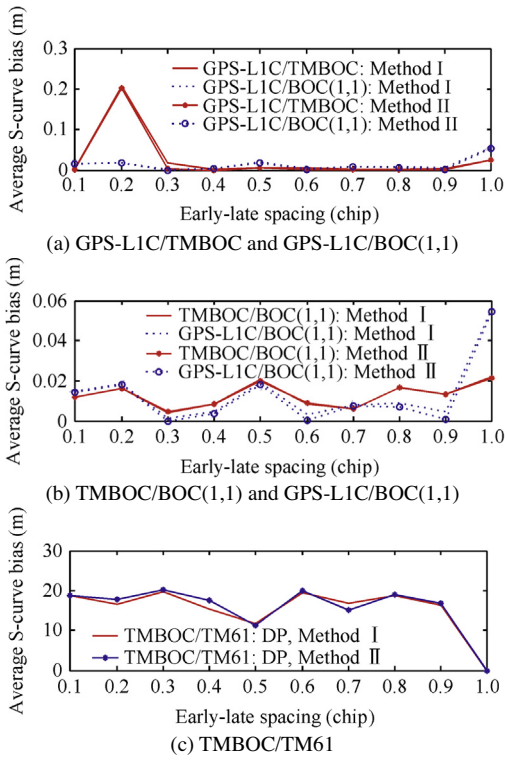

Fig. 14 Comparison of average S-curve biases obtained by using different optimization methods for GPS L1C.

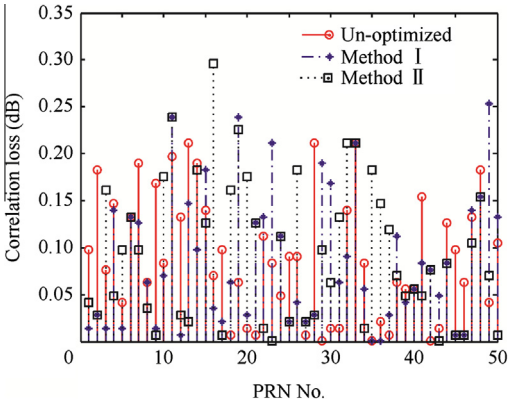

Fig. 15 Correlation loss due to data and pilot codes cross-correlation: Galileo E1 OS.

the optimized pairs provide similar correlation losses to the un-optimized pairs for total Galileo E1 OS signals, which can be demonstrated by the average correlation loss. The average value of correlation loss is 0.091 dB, 0.087 dB and 0.094 dB for the pairs un-optimized, optimized by Method I and optimized by Method II, respectively. The correlation loss of un-optimized and optimized data/pilot code pairs for GPS-L1C/TMBOC, are illustrated in Fig. 16. For GPS L1C, the average value of correlation loss is 0.012 dB, 0.013 dB and 0.012 dB for the pairs un-optimized, optimized by Method I and optimized by Method II, respectively. It is clear that the difference of correlation losses between un-optimized and optimized pairs is very small. Considering the magnitude of the average correlation loss, the SNR loss and the detection performance degradation caused by codes correlation for optimized pairs are negligible.

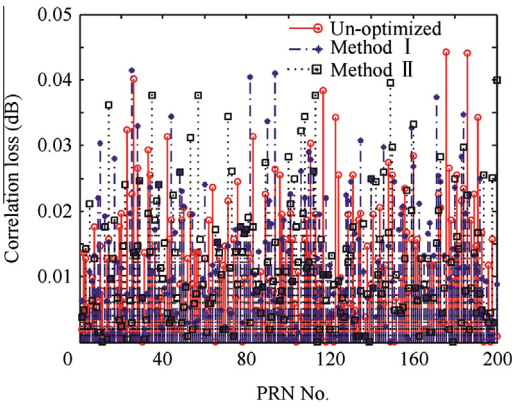

Fig. 16 Correlation loss due to data and pilot codes cross-correlation: GPS L1C.

4.3.2. Code tracking variance

Assuming that the impact of codes cross-correlation is negligible, the code tracking variance in the presence of thermal noise with a non-coherent DP discriminator is given by[16]

$$\sigma^2_{\mathrm{DP}} = \frac{B_{\mathrm{L}}(1-0.5B_{\mathrm{L}}T_{\mathrm{I}})\int_{-B_{\mathrm{W}}}^{B_{\mathrm{W}}} G_c(f)\sin^2(\pi f\Delta)\mathrm{d}f}{\frac{C}{N_0}\times\left(2\pi\int_{-B_{\mathrm{W}}}^{B_{\mathrm{W}}} fG_c(f)\sin(\pi f\Delta)\mathrm{d}f\right)^2} \times\left(1+\frac{N_0/C}{T_{\mathrm{I}}\int_{-B_{\mathrm{W}}}^{B_{\mathrm{W}}} G_c(f)\mathrm{d}f}\right) \quad (36)$$

where B_{W}, B_{L}, $\mathrm{T_I}$, and C/N_0 are the pre-correlation bandwidth, loop bandwidth, integration time and the carrier-to-noise density ratio, respectively. $G_c(f)$ is the power spectral density (PSD) function of $c(t)$, which is the Fourier transform of $R_c(\tau)$.

In order to assess the code tracking performance of un-optimized and optimized data/pilot code pairs in the presence of thermal noise, the Monte Carlo simulations are carried out for Galileo E1 OS and GPS L1C signals. In the following code tracking variance estimations, the code loop bandwidth B_{L} = 1 Hz, the pre-correlation bandwidth (double-sided) $2B_{\mathrm{W}}$ = 50 MHz, the early-late spacing Δ = 0.4 chip, and the integration time (T_{I}) is 4 ms and 10 ms for Galileo E1 OS and Galileo L1C, respectively.

Comparisons of the standard deviations of code tracking error (i.e., the square root of code tracking variance) between un-optimized and optimized code pairs for CBOC/CBOC(−) and GPS-L1C/TMBOC are depicted in Figs. 17 and 18, respectively. The curves indicated by 'Theory' can be easily obtained from Eq. (36). Other curves are the average code tracking errors of all code pairs for different tracking algorithms, which are obtained by Monte Carlo simulations. For both Galileo E1 OS and GPS L1C, the un-optimized code pairs show poorer noise performance than the optimized code pairs, due to the impact of codes cross-correlation. On the other hand, the code pairs optimized by Method I and Method II provide very similar code tracking performance in the presence of thermal noise.

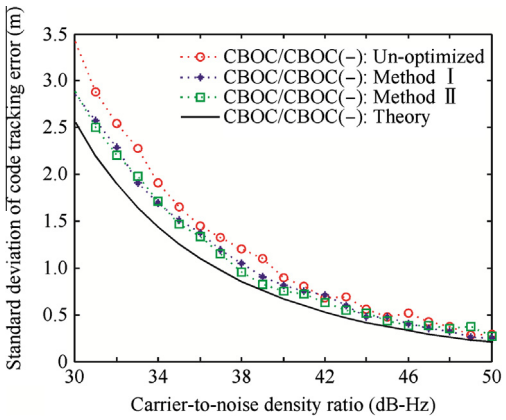

Fig. 17 Standard deviations of code tracking error due to thermal noise for CBOC/CBOC(−).

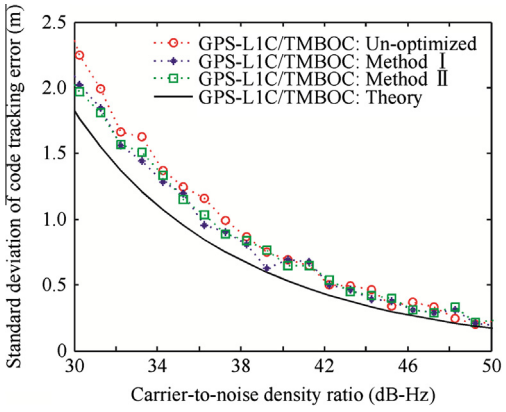

Fig. 18 Standard deviations of code tracking error due to thermal noise for GPS-L1C/TMBOC.

5. Conclusions

(1) The impact of data and pilot PRN codes cross-correlation on the S-curve bias for Galileo E1 OS and GPS L1C has been presented in this paper. When only the pilot components are tracked, GPS L1C provides smaller average S-curve bias, as compared to Galileo E1 OS, due to the difference in the code length and the power proportion between data and pilot components. It can be noted that, for CBOC signals, the data channels provide improvement of the resistance to the codes cross-correlation with respect to the pilot channels. The S-curve bias can be magnified by an inappropriate choice of the early-late spacing, leading to noticeable worsening in receiver performance. Considering the S-curve bias, the reception of MBOC signals with the BOC(1,1) receiver is recommendable, especially for the market applications. However, it seems inappropriate to apply the TM61 method to MBOC signals tracking.

(2) Two methods are proposed to optimize the data/pilot PRN code pairs. The code pairs optimized by using both methods significantly decrease the codes cross-correlation, as compared to the un-optimized code pairs. As for Galileo E1 OS, Method II outperforms Method I for all tracking algorithms and early-late spacings considered. For GPS L1C, the codes cross-correlation mitigation of method II is not so significant over method I. Moreover, GPS L1C seems to be more sensitive to the optimization parameters (e.g., the early-late spacing assumed in the optimization). It should be noted that the optimization criterion may not be unique (e.g., changing the early-late spacing). Different results could be expected upon using other optimization criteria, especially for GPS L1C. For both Galileo E1 OS and GPS L1C, the proposed code pairs show better noise performance than the original pairs, due to the reduction of codes cross-correlation. However, the difference between the original and proposed pairs in terms of correlation loss is negligible.

(3) Analyses in this paper show that the currently published data and pilot PRN codes of Galileo E1 OS and GPS L1C could still be further optimized to mitigate the codes cross-correlation, and thus further improvement in code tracking performance is still achievable in this regard.

(4) Finally, it can be concluded that the intra-channel (data and pilot) codes cross-correlation would be an important criterion for PRN codes design, especially when data and pilot components are transmitted in phase. Furthermore, the modulation characteristics of data and pilot signals should be considered. As for the complexity in PRN codes design, it is advisable to transmit the data and pilot components in quadrature (e.g., the GPS L5 signal), or multiplex the data and pilot components in time domain (e.g., the GPS L2C signal) for future GNSS signals.

Acknowledgment

This study was supported by National Basic Research Program of China (No. 2010CB731805).

References

1. United States and the European Union announce final design for GPS-Galileo common civil signal. http://europa.eu/rapid/pressReleasesAction.do?reference=IP/07/1180&format=HTML&aged=1&language=EN&guiLanguage=en [retrieved 20.11.11].
2. IS-GPS-800A. *NAVSTAR global positioning system space segment/user segment L1C interface*. El Segundo, CA: Science Applications International Corporation; 2010.
3. Galileo open service signal in space interface control document (OS SIS ICD), issue 1.1. Brussels, Belgium: European Union; 2010.
4. Hein GW, Avila-Rodriguez JA, Wallner S. The DaVinci Galileo code and others. *Inside GNSS* 2006;**1**(6):62–74.
5. Winkel J. *Spreading codes for a satellite navigation system*. US Patent No. 8,035,555, 2011.
6. Rushanan JJ. The spreading and overlay codes for the L1C signal. *Navigation* 2007;**54**(1):43–51.
7. Rushanan JJ. Weil sequences: a family of binary sequences with good correlation properties. In: *IEEE international symposium on information theory*, 2006. p. 1648–52.

8. Soualle F, Soellner M, Wallner S. Spreading code selection criteria for the future GNSS Galileo. In: *Proceedings of the European navigation conference GNSS 2005*, 2005.
9. Wallner S, Avila-Rodriguez JA, Hein GW, Galileo E1 OS and GPS L1C pseudo random noise codes—requirements, generation, optimization and comparison. In: *Proceedings of the international technical meeting of the institute of navigation*, 2007. p. 1549–63.
10. Margaria D, Savasta S, Dovis F. Codes cross-correlation impact on the interference vulnerability of Galileo E1 OS and GPS L1C signals. In: *Proceedings of the 2010 international technical meeting of the institute of navigation*, 2010. p. 941–51.
11. Motella B, Savasta S, Margaria D. Method for assessing the interference impact on GNSS receivers. *IEEE Trans Aerosp Electron Syst* 2011;**47**(2):1416–32.
12. Wallner S, Avila-Rodriguez JA, Won JH. Revised PRN code structures for Galileo E1 OS. In: *Proceedings of the 21st international technical meeting of the satellite division of the institute of navigation*, 2008. p. 887–99.
13. Hein GW, Avila-Rodriguez JA, Wallner S. MBOC: the new optimized spreading modulation recommended for Galileo L1 OS and GPS L1C. *Inside GNSS* 2006;**1**(4):57–65.
14. Kacmarik P, Kovar P. GNSS signals characteristics. In: *Proceedings of 17th international conference radioelektronika*, 2007. p. 199–204.
15. Soellner M, Kurzhals C, Hechenblaikner G. GNSS offline signal quality assessment. In: *Proceedings of the 21st international technical meeting of the satellite division of the institute of navigation*, 2008. p. 909–20.
16. Julien O. Design of Galileo L1F receiver tracking loops. Ph.D. Thesis, University of Calgary, 2005.
17. Lohan ES. Analytical performance of CBOC-modulated Galileo E1 signal using sine BOC(1,1) receiver for mass-market applications. In: *Proceedings of IEEE/ION position, location, and navigation symposium (PLANS)*, 2010. p. 245–53.
18. Julien O, Macabiau C, Issler JL. 1-Bit processing of composite BOC (CBOC) signals and extension to time-multiplexed BOC (TMBOC) signals. In: *Proceedings of the 2007 national technical meeting of the institute of navigation*, 2007. p. 227–39.
19. Fantino M, Mulassano P, Dovis F. Performance of the proposed Galileo CBOC modulation in heavy multipath environment. *Wirel Pers Commun* 2008;**44**(3):323–39.
20. Hillier FS, Lieberman GJ. *Introduction to operations research*. 7th ed. New York: McGraw-Hill; 2002.
21. Taha HA. *Operations research: an introduction*. 8th ed. New Jersey: Prentice Hall; 2007.

Yang Zaixiu is a Ph.D. student in the school of Electronic and Information Engineering at Beihang University. His area of research includes GNSS signals processing and performance assessment.

Huang Zhigang received his Ph.D. degree from Beihang University in 2002. Now he is a professor in the School of Electronic and Information Engineering at Beihang University. His research interests include radio navigation and satellite navigation.

Geng Shengqun received his Ph.D. degree from Beijing Institute of Technology in 2005. Now he is an instructor in the School of Electronic and Information Engineering at Beihang University. His research areas include satellite navigation receiver and simulator design.